JOURNAL OF AGRICULTURAL AND FOOD CHEMISTRY

Carcinogenicity of Acrylamide: A Computational Study

KATJA GALEŠA,[†,‡] URBAN BREN,[†,‡] AGATA KRANJC,[§] AND JANEZ MAVRI*[,‡]

National Institute of Chemistry, Hajdrihova 19, SI-1001 Ljubljana, Slovenia, and International School for Advanced Studies (SISSA/ISAS), via Beirut 2-4, I-34014 Trieste, Italy

This paper reports a series of ab initio, density functional theory (DFT), and semiempirical molecular orbital (MO) calculations concerning the reaction between the ultimate carcinogen of acrylamide and guanine. Acrylamide—a product of the Maillard reaction—is present in a variety of fried and oven-cooked food. After intake, it is epoxidized by cytochrome P450 2E1 to yield the ultimate carcinogen—glycidamide. Effects of solvation were considered using the Langevin dipoles (LD) model of Florian and Warshel and the solvent reaction field (SCRF) model of Tomasi and co-workers. In silico activation free energies are in very good agreement with the experimental value of 22.8 kcal/mol. This agreement presents strong evidence in favor of the validity of the proposed S_N2 reaction mechanism and points to the applicability of quantum chemical methods to studies of reactions associated with carcinogenesis. In addition, insignificant stereoselectivity of the studied reaction was predicted. Finally, the competing reaction of glycidamide with adenine was simulated, and the experimentally observed regioselectivity was successfully reproduced.

KEYWORDS: Carcinogenicity; acrylamide; DNA alkylation; activation free energy; quantum chemical calculations; solvation effects

INTRODUCTION

Acrylamide is of great biological interest due to its role in the etiology of cancer (*1*). In 2002 its presence in a variety of fried and oven-cooked food was discovered (*2*). Acrylamide is generated as a result of Maillard reaction from asparagine—a major amino acid in potato and cereals—and reducing sugars during heat treatment (*3*). Human dietary exposure to acrylamide is not negligible and can amount to 100 μg per day (*4*). In addition, industrial workers in the manufacture of paper or in the production of water soluble polymers are exposed to acrylamide through inhalation and grout workers through skin absorption (*5, 6*).

Acrylamide is metabolized in vivo through conjugation with glutathione (*7, 8*) or through epoxidation by cytochrome P450 2E1 (*9*) to glycidamide (*10, 11*). Glycidamide is considered to be the ultimate carcinogen of acrylamide, because it alkylates DNA mainly at the N7 position of guanine (*12, 13*). The proposed reaction mechanism leading to the formation of the N7-(2-carbamoyl-2-hydroxyethyl)guanine DNA adduct is depicted in **Figure 1**. The S_N2 substitution represents the rate-limiting step of the reaction. Subsequent protonation is believed to be a fast process due to a proton-rich microenviroment surrounding DNA (*14*). This alkylation is followed by other reactions, of which depurination—leading to gene mutations and chromosomal aberrations—is a typical example. In addition, glycidamide was also found to alkylate DNA at the N3 position of adenine (*13, 15*), although in around 100-fold lower amount (*16*). The proposed reaction mechanism leading to the formation of the N3-(2-carbamoyl-2-hydroxyethyl)adenine DNA adduct is presented in **Figure 2**. Moreover, a small quantity of N1-(2-carboxy-2-hydroxyethyl)adenine DNA adduct was detected in vitro but surprisingly not in vivo (*13*). **Figure 3** depicts the proposed reaction mechanism leading to its formation. Finally, acrylamide was also found to directly alkylate DNA via Michael addition as presented for the case of guanine in **Figure 4** (*17, 18*). This reaction is presumably much slower, although its kinetics and regioselectivity are yet to be explored.

Chronic acrylamide exposure was shown to produce tumors in rats (*19, 20*). Some suggestions have been made for a hormone-mediated mechanism of acrylamide carcinogenicity (*21*), but evidence of a genotoxic mechanism involving glycidamide-derived DNA adducts is much more convincing (*12*).

In this study, activation free energies $\Delta G^{\ddagger}$ of the reaction between glycidamide and guanine, calculated at several ab initio, density functional theory (DFT), and semiempirical molecular

* Author to whom correspondence should be addressed (e-mail janez@kihp2.cmm.ki.si; telephone +386-1-4760309; fax +386-1-4760300).

† K.G. and U.B. contributed equally to this work.

‡ National Institute of Chemistry.

§ International School for Advanced Studies (SISSA/ISAS).

10.1021/jf800965y CCC: $40.75
Published on Web 08/23/2008

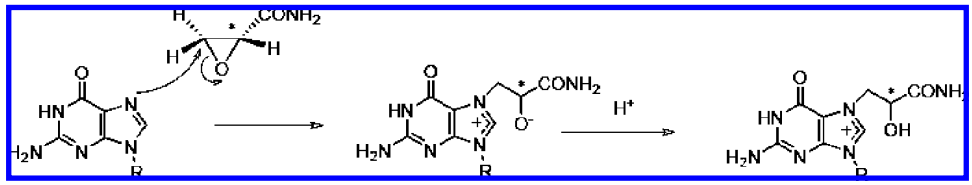

Figure 1. Proposed mechanism of the reaction between glycidamide and guanine giving rise to the N7-(2-carbamoyl-2-hydroxyethyl)guanine adduct.

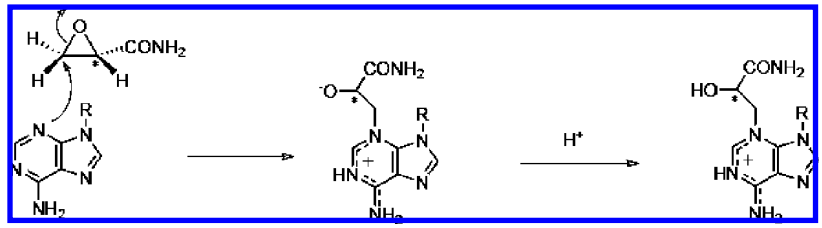

Figure 2. Proposed mechanism of the reaction between glycidamide and adenine leading to the N3-(2-carbamoyl-2-hydroxyethyl)adenine adduct.

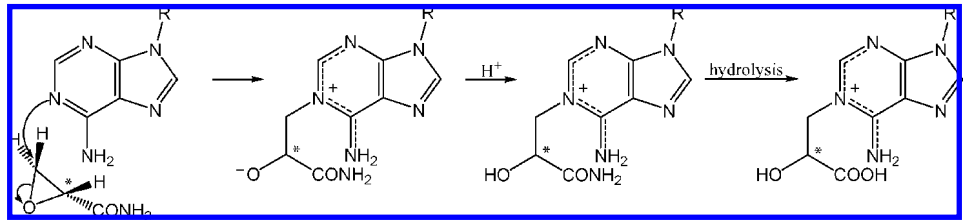

Figure 3. Proposed mechanism of the reaction between glycidamide and adenine giving rise to the N1-(2-carboxy-2-hydroxyethyl)adenine adduct.

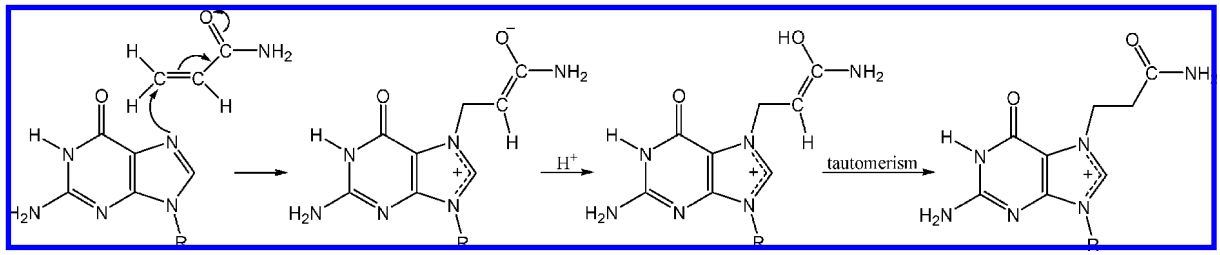

Figure 4. Proposed mechanism of the reaction between acrylamide and guanine leading to the N7-(2-formamidoethyl)guanine adduct.

orbital (MO) levels, are compared to the experimental free energy barrier. Its value of 22.8 kcal/mol was obtained from the experimentally determined rate constant k (*22*) on the basis of the transition state theory

$$k = \frac{k_B T}{h} \times e^{-\frac{\Delta G^{\ddagger}}{k_B T}} \quad (1)$$

where k_B represents Boltzmann constant, h the Planck constant, and T the absolute temperature. Transition state theory is based on the assumption that reactants and transition states form a thermal equilibrium. Its validity in biocatalysis was proven experimentally by the development of catalytic antibodies and theoretically by the success of the empirical valence bond (EVB) method (*23*).

Because biochemical reactions do not take place in vacuo, solvation effects had to be incorporated by the solvent reaction field method of Tomasi and co-workers (*24*) and the Langevin dipole model of Florian and Warshel (*25*). In addition, hydration effects in conjunction with the semiempirical MO methods were studied at the AM1-SM1 and PM3-SM3 levels (*26*).

COMPUTATIONAL METHODS

All calculations were performed at the National Institute of Chemistry in Ljubljana on the CROW 9 cluster (*27, 28*) consisting of 64 Linux-based personal computers running two AMD Opteron processors at 1.6 GHz. To obtain the Born−Oppenheimer (BO) hypersurface for the reaction between acrylamide and guanine, a series of ab initio, DFT, and semiempirical MO simulations was performed with the Gaussian 03 suite of programs (*29*). For the reactants a full geometry optimization was applied. The transition state structure was located with the Berny algorithm. The difference between energies of the transition state and the reactants is activation energy. Moreover, vibrational analysis in the harmonic approximation was performed, and only real frequencies for the reactants and a single imaginary frequency for the transition state were obtained at all levels of theory.

Calculation of the Born−Oppenheimer surface for chemical reactions is not a trivial task. It is generally accepted that one needs relatively flexible basis sets and adequate treatment of electron correlation. The ab initio calculations were performed on the Hartree−Fock (HF) level in conjunction with the 6-31G(d), 6-31+G(d,p), and 6-311++G(d,p) basis sets and on the MP2 (Møller−Plesset perturbation of the second order) level of theory in combination with the 6-31G(d), 6-31+G(d), and 6-31+G(d,p) basis sets. In addition, we considered the DFT method B3LYP that has exchange functional introduced by Becke (*30*) combined with the correlation functional of Lee, Yang, and Parr (*31*). Basis sets 6-31G(d), 6-31+G(d,p), and 6-311++G(d,p) were again applied. We are aware of the significant empirical character of the DFT methods, but they do to some extent include the electron correlation. Finally, we

Table 1. Activation Energies for the Reaction between Glycidamide and Guanine Calculated with Different Methods

method	$\Delta E^{\ddagger a}$ (kcal/mol)	ZPE^{TSb} (kcal/mol)	ZPE^{Rc} (kcal/mol)	ΔZPE^{d} (kcal/mol)	ω^{TSe} (i cm^{-1})	ω^{Rf} (cm^{-1})	d^{TSg} (Å)	d^{Rh} (Å)
AM1	46.40	145.86	146.94	−1.08	782	5.62	1.87	3.14
PM3	38.46	140.10	140.39	−0.29	757	4.88	1.89	3.99
HF/6-31G(d)	39.39	156.74	156.93	−0.19	578	15.11	1.93	3.17
HF/6-31+G(d,p)	37.62	155.76	156.04	−0.28	562	16.74	1.96	3.25
HF/6-311++G(d,p)	37.97	155.01	155.25	−0.24	559	15.66	1.97	3.27
B3LYP/6-31G(d)	27.19	144.81	145.07	−0.26	418	15.23	1.90	3.11
B3LYP/6-31+G(d,p)	25.84	144.07	144.38	−0.31	416	16.50	1.93	3.20
B3LYP/6-311++G(d,p)	25.68	143.52	143.81	−0.29	407	14.80	1.94	3.20
MP2/6-31G(d)	38.03	146.62	146.75	−0.12	567	14.65	1.84	2.99
MP2/6-31+G(d)	35.61	145.51	145.55	−0.04	555	8.06	1.88	3.23
MP2/6-31+G(d,p)	35.67	146.12	146.05	−0.07	558	9.86	1.88	3.22

[a] Gas-phase activation energy. [b] Zero-point vibrational energy for the transition state. [c] Zero-point vibrational energy for the reactants. [d] Zero-point energy of the transition state minus zero-point energy of the reactants. [e] Imaginary frequency value corresponding to the transition state. [f] The lowest frequency value corresponding to the reactant structure. [g] Distance between the N7 atom of guanine and the nonchiral carbon of glycidamide for the transition state. [h] Distance between the N7 atom of guanine and the nonchiral carbon of glycidamide for the reactant structure.

Table 2. Activation Free Energies for the Reaction between Glycidamide and Guanine Calculated by the Solvent Reaction Field (SCRF) Method

method	$\Delta G_{hydr}^{SCRF}(TS)^{a}$ (kcal/mol)	$\Delta G_{hydr}^{SCRF}(R)^{b}$ (kcal/mol)	$\Delta\Delta G_{hydr}^{SCRFc}$ (kcal/mol)	$\Delta G^{\ddagger}{}_{SCRF}{}^{d}$ (kcal/mol)
HF/6-31G(d)	−29.87	−18.99	−10.88	28.32
HF/6-31+G(d,p)	−34.16	−22.29	−11.87	25.47
HF/6-311++G(d,p)	−33.37	−21.42	−11.95	25.78
B3LYP/6-31G(d)	−25.04	−16.04	−9.03	17.90
B3LYP/6-31+G(d,p)	−30.93	−20.60	−10.33	15.20
B3LYP/6-311++G(d,p)	−30.60	−20.01	−10.59	14.80
MP2/6-31G(d)	−32.38	−20.21	−12.17	25.74
MP2/6-31+G(d)	−37.28	−23.57	−13.71	21.86
MP2/6-31+G(d,p)	−37.01	−23.53	−13.48	22.12
exptl value				22.8

[a] Hydration free energy for the transition state obtained by the SCRF method. [b] Hydration free energy for the reactants calculated by the SCRF method. [c] Hydration free energy of the transition state minus hydration free energy of the reactants. [d] Activation free energy.

used the semiempirical MO methods AM1 and PM3 due to their low CPU cost, which allows for their application in QM/MM methodology in conjunction with thermal averaging and calculation of nuclear quantum effects (*32*).

Hydration free energies for reactants and the transition state were calculated with two methods, the solvent reaction field (SCRF) of Tomasi and co-workers (*24*) and the Langevin dipoles model (LD) parametrized by Florian and Warshel (*25*). The SCRF method encoded in the Gaussian 03 package was applied at all ab initio and DFT levels. Obtained Merz−Kollman partial atomic charges served as an input for LD model built in the ChemSol program (*33*). The AM1-SM1 and PM3-SM3 calculations were performed by the AMSOL-5.4.1 program of Truhlar and co-workers (*26*).

RESULTS AND DISCUSSION

The calculated activation energies, zero-point energies, and imaginary frequencies of transition state structures for the reaction between glycidamide and guanine are collected in **Table 1**. Hydration free energies obtained by the solvent reaction field method are presented in **Table 2**. Solvation free energies calculated with the LD model are collected in **Table 3**. The AM1-SM1- and PM3-SM3-based hydration free energies are shown in **Table 4**. **Tables 2−4** also include activation free energies calculated as

Table 3. Activation Free Energies for the Reaction between Glycidamide and Guanine Calculated by the Langevin Dipoles (LD) Method

method	$\Delta G_{hydr}^{LD}(TS)^{a}$ (kcal/mol)	$\Delta G_{hydr}^{LD}(R)^{b}$ (kcal/mol)	$\Delta\Delta G_{hydr}^{LDc}$ (kcal/mol)	$\Delta G^{\ddagger}{}_{LD}{}^{d}$ (kcal/mol)
HF/6-31G(d)	−43.18	−31.00	−12.18	27.02
HF/6-31+G(d,p)	−47.80	−33.98	−13.82	23.52
HF/6-311++G(d,p)	−47.55	−33.37	−14.18	23.55
B3LYP/6-31G(d)	−39.56	−28.69	−10.87	16.06
B3LYP/6-31+G(d,p)	−45.98	−33.09	−12.89	12.64
B3LYP/6-311++G(d,p)	−45.67	−32.55	−13.12	12.27
exptl value				22.8

[a] Hydration free energy for the transition state obtained by the LD method. [b] Hydration free energy for the reactants calculated by the LD method. [c] Hydration free energy of the transition state minus hydration free energy of the reactants. [d] Activation free energy.

Table 4. Activation Free Energies for the Reaction between Glycidamide and Guanine Calculated by the AM1-SM1 and PM3-SM3 Methods

method	$\Delta G_{hydr}(TS)^{a}$ (kcal/mol)	$\Delta G_{hydr}(R)^{b}$ (kcal/mol)	$\Delta\Delta G_{hydr}{}^{c}$ (kcal/mol)	$\Delta G^{\ddagger d}$ (kcal/mol)
AM1-SM1	−36.03	−29.33	−6.70	38.61
PM3-SM3	−45.88	−40.31	−5.57	32.60
exptl value				22.8

[a] Hydration free energy for the transition state obtained by the AM1-SM1 and PM3-SM3 methods. [b] Hydration free energy for the reactants calculated by the AM1-SM1 and PM3-SM3 methods. [c] Hydration free energy for the transition state minus hydration free energy for the reactants. [d] Activation free energy.

$$\Delta G^{\ddagger} = \Delta E^{\ddagger} + \Delta ZPE + \Delta\Delta G_{hydr} \quad (2)$$

where $\Delta E^{\ddagger}$ represents the activation energy of the gas phase reaction, ΔZPE denotes the relative zero-point energy of the transition state and the reactants, and $\Delta\Delta G_{hydr}$ stands for the corresponding relative hydration free energy. The entropic contribution is frequently calculated as the sum of translational, rotational, and vibrational entropies obtained using the ideal gas, rigid rotor, and harmonic oscillator approximations (*34*). However, it has been argued that the use of these approximations often leads to a dramatic overestimation of the entropy term for reactions in solution (*35*). The most important reason for the observed overestimation lies in the fact that the harmonic approximation underestimates the entropy contribution from the low-frequency modes that are more abundant in larger solutes.

Therefore, solvation entropies included in relative solvation free energies present the correct treatment of entropic contribution for reactions in solution (*36*).

Our calculations focus on the first step of the reaction between glycidamide and guanine (**Figure 1**) as this S_N2 substitution represents the rate-limiting step. It leads to the formation of the relatively unstable zwitterionic intermediate with tetrahedral coordination of the chiral carbon atom. The activation free energy is defined as a free energy difference between the transition state and the reactants. To obtain the activation free energy of this first step, we therefore need only to consider its reactants (glycidamide + guanine in **Figure 1**) and its transition state—the saddle point characterized by a single imaginary frequency on the potential energy surface connecting reactants and the zwitterionic intermediate. The subsequent protonation step is a fast process due to a proton-rich microenvironment surrounding DNA (*14*).

From activation energies for the reaction between glycidamide and guanine collected in **Table 1** it is evident that the convergence in terms of basis set size was reached at all levels of theory. The addition of diffuse and polarization functions on heavy atoms is crucial for obtaining the converged barrier in terms of the basis set size. The predicted reaction barrier at the Hartree−Fock level lies between 37 and 40 kcal/mol. Almost identical activation energies were obtained at the MP2 level. These calculations were very demanding due to the large size of the studied system. DFT calculations drastically reduce the reaction barrier, whereas the semiempirical MO method AM1 increases it. By using the semiempirical MO method PM3, which was demonstrated to yield reasonable energetics for the reaction catalyzed by xylose isomerase (*32*), an activation energy similar to the HF level was obtained.

The zero-point vibrational energy correction of the reaction barrier is practically negligible (**Table 1**). In addition, it should be noted that the DFT- and MP2-calculated BO surfaces are shallower than the HF-calculated ones. This fact is reflected in the absolute values of the zero-point vibrational energies. A single imaginary vibrational frequency was obtained for the transition state structure at all theory levels (**Table 1**). Vibration modes of these imaginary frequencies were visualized by means of MOLDEN program (*37*), because they should correspond to the reaction coordinate of the first step of the reaction mechanism depicted in **Figure 1**. At all levels of theory the vibration mode of the imaginary frequency coincided with the formation of a chemical bond between the N7 atom of guanine and the nonchiral carbon of glycidamide and with the cleavage of the chemical bond connecting this nonchiral glycidamide carbon to the epoxide oxygen, thus confirming the allocation of the correct transition state structure. The vibration mode of the imaginary frequency obtained at the MP2/6-31+G(d,p) level of theory can be viewed as movie 1 included in the Supporting Information. The structures of the reactants and the transition state for the reaction between glycidamide and guanine calculated at the MP2/6-31+G(d,p) level of theory are presented in **Figure 5**.

In **Table 2** we collected hydration free energies calculated by the solvent reaction field method of Tomasi and co-workers (*24*). The solvent accelerates the reaction because the transition state is better solvated than the reactants. This finding reflects the formation of the zwitterionic intermediate in the first step of the reaction between glycidamide and guanine (**Figure 1**). Reduction of the reaction barrier in terms of the relative hydration free energies is largest for MP2 methods and smallest for DFT methods. All in all, the MP2 level of theory in conjunction with the SCRF model and flexible basis sets gives activation free energies that are in very good agreement with the experimental value of 22.8 kcal/mol. HF reaction barriers are moderately overestimated, and DFT reaction barriers are significantly underestimated.

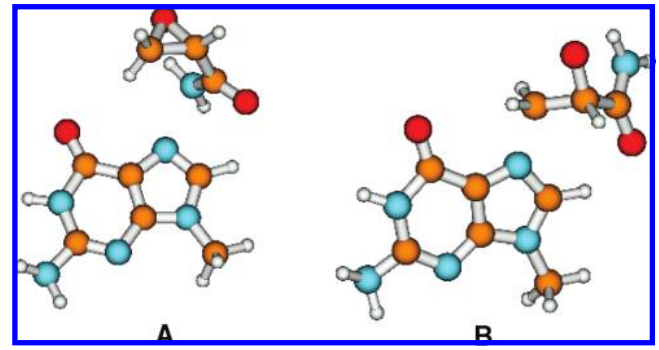

Figure 5. Structures of the reactants (**A**) and the transition state (**B**) for the guanine alkylation by glycidamide calculated at the MP2/6-31+G(d,p) level of theory. Oxygen is depicted in red, carbon in orange, nitrogen in blue, and hydrogen in white.

All presented results were obtained for the *R* stereoisomer of glycidamide (**Figure 1**). To check for the stereoselectivity of the reaction between glycidamide and guanine, the activation free energy was recalculated for the *S* stereoisomer of glycidamide using the SCRF model at the HF/6-31G(d) level of theory. The reaction barriers were 28.32 and 28.33 kcal/mol for the *R* and *S* stereoisomers, respectively, thus making the stereoselectivity of the reaction insignificant. This fact can be easily understood in view of the nearly planar character of guanine. Inclusion of the whole DNA may somewhat increase this steroselectivity.

Table 3 shows hydration free energies calculated by the Langevin dipoles solvation model. Reduction of the reaction barrier in terms of the relative hydration free energies is more pronounced than in the SCRF model. Again, a larger reduction is obtained for HF methods than for DFT methods. The HF level of theory in conjunction with the LD solvation model and flexible basis sets yields activation free energies that are in very good agreement with the experimental data. DFT calculations significantly underestimate the reaction barrier.

Table 4 presents the results obtained by semiempirical MO methods in conjunction with solvation models of Cramer and Truhlar (*38, 39*)—AM1-SM1 and PM3-SM3. Reduction of the reaction barrier in terms of the relative hydration free energies is less pronounced than in the SCRF or LD model. Therefore, both levels of theory significantly overestimate the activation free energy of the reaction between glycidamide and guanine.

All in all, the B3LYP functional regardless of the applied solvation model or basis set systematically underestimates the activation free energy of the reaction between glycidamide and guanine. To determine which solvation model outperforms the others, a series of hydration free energy calculations on optimized structures of adenine and guanine was carried out (**Table 5**) and compared to the results of the available free energy perturbation studies using molecular dynamics simulations and explicit solvent (*40*−*42*). As both SCRF in conjunction with MP2/6-31G(d) level of theory and LD in combination with B3LYP/6-31G(d) level of theory provide good agreement, we cannot claim which solvation model performs better. However, in contrast to the solvent reaction field the Langevin dipoles do to a certain extent involve thermal averaging and specific interactions between solute and solvent. The discrepancy between the hydration free

Table 5. Hydration Free Energies of Adenine and Guanine Calculated with Different Methods

method	ΔG_{hydr}[a](adenine) (kcal/mol)	ΔG_{hydr}[b](guanine) (kcal/mol)
AM1-SM1	−23.19	−27.81
PM3-SM3	−24.38	−30.52
SCRF HF/6-31G(d)	−7.61	−21.36
SCRF B3LYP/6-31G(d)	−5.72	−18.48
SCRF MP2/6-31G(d)	−8.46	−22.92
LD HF/6-31G(d)	−12.13	−27.58
LD B3LYP/6-31G(d)	−11.25	−25.34
AMBER/FEP[c]	−11.65	−22.65

[a] Hydration free energy of adenine calculated with different methods. [b] Hydration free energy of guanine calculated with different methods. [c] Free energy perturbation in conjunction with AMBER force field and explicit solvent (*40*).

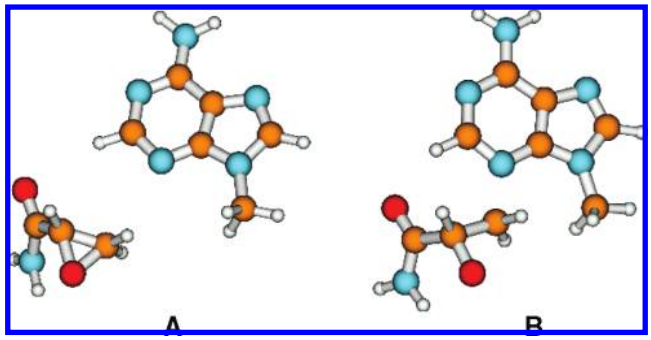

Figure 6. Structures of the reactants (**A**) and the transition state (**B**) for the N3 adenine alkylation by glycidamide calculated at the MP2/6-31+G(d) level of theory. Oxygen is depicted in red, carbon in orange, nitrogen in blue, and hydrogen in white.

energies obtained by both solvation models could be rationalized by the fact that there were no epoxy species or zwitterions used in their parametrization sets (*25, 43*).

The competing reaction between adenine at the N3 position and glycidamide depicted in **Figure 2** was simulated as well. Calculations at the MP2 level of theory in conjunction with flexible basis set 6-31+G(d) and the SCRF model (which yielded a very good agreement with the experimental free energy barrier in the case of guanine) gave an activation energy of 36.47 kcal/mol, a zero-point energy correction of −0.08 kcal/mol, a hydration free energy correction of −9.87 kcal/mol, and consequently the activation free energy of 26.52 kcal/mol. Therefore, reaction between glycidamide and guanine is preferred by 4.66 kcal/mol and should, according to the transition state theory, proceed around 1000 times more rapidly than the competing reaction between glycidamide and adenine. This result is in accordance with the tissue analysis of rats exposed to acrylamide, which showed that the N7-(2-carbamoyl-2-hydroxyethyl)guanine DNA adduct is formed in around 100 times larger amount than the N3-(2-carbamoyl-2-hydroxyethyl)adenine adduct (*16*). The structures of the reactants and the transition state for the reaction between glycidamide and adenine calculated at the MP2/6-31+G(d) level of theory are presented in **Figure 6**. A single imaginary vibrational frequency was obtained for the transition state structure. Its vibration mode coincided with the reaction coordinate of the first step of the reaction mechanism depicted in **Figure 2**—the formation of a chemical bond between the N3 atom of adenine and the nonchiral carbon of glycidamide and with the cleavage of the chemical bond connecting this nonchiral glycidamide carbon

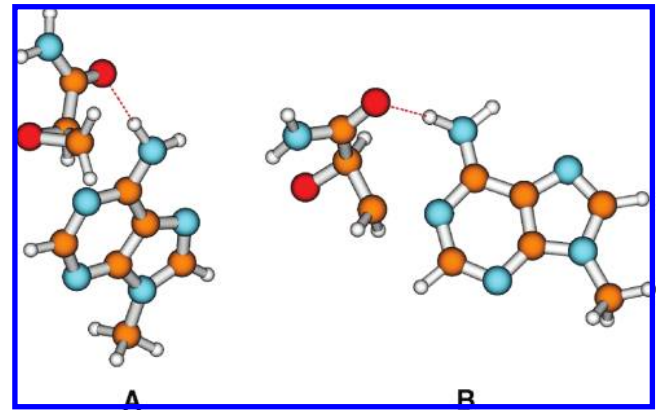

Figure 7. Structures of the reactants (**A**) and the transition state (**B**) for the N1 adenine alkylation by glycidamide calculated at the MP2/6-31+G(d) level of theory. Oxygen is depicted in red, carbon in orange, nitrogen in blue, and hydrogen in white.

to the epoxide oxygen—thus confirming the allocation of the correct transition state structure. The vibration mode of the imaginary frequency obtained at the MP2/6-31+G(d) level of theory can be viewed as movie 2 included in the Supporting Information.

In addition, the reaction between adenine at the N1 position and glycidamide depicted in **Figure 3** was simulated—again at the MP2 level of theory in conjunction with flexible basis set 6-31+G(d) and the SCRF model. Calculation yielded an activation energy of 40.66 kcal/mol, a zero-point energy correction of −0.17 kcal/mol, a hydration free energy correction of −13.01 kcal/mol, and consequently the activation free energy of 27.48 kcal/mol. Therefore, according to the transition state theory the N1-(2-carboxy-2-hydroxyethyl)adenine DNA adduct should be formed in about 5 times lower amount than its N3 regioisomer. On the other hand, a caveat has to be issued that the N1 atom of adenine is directly involved in Watson−Crick pairing with the neighboring thymine, thereby sterically hindering glycidamide alkylation. N1-(2-carboxy-2-hydroxyethyl)adenine DNA adduct formation should, therefore, be extremely susceptible to DNA denaturation, which might explain why such an adduct was detected in vitro but not in vivo (*13*). The structures of the reactants and the transition state for the reaction between glycidamide and adenine calculated at the MP2/6-31+G(d) level of theory are presented in **Figure 7**. A single imaginary vibrational frequency was obtained for the transition state structure. Its vibration mode coincided with the reaction coordinate of the first step of the reaction mechanism depicted in **Figure 3**—the formation of a chemical bond between the N1 atom of adenine and the nonchiral carbon of glycidamide and with the cleavage of the chemical bond connecting this nonchiral glycidamide carbon to the epoxide oxygen—thus confirming the allocation of the correct transition state structure. The vibration mode of the imaginary frequency obtained at the MP2/6-31+G(d) level of theory can be viewed as movie 3 included in the Supporting Information.

Finally, we simulated direct reaction between acrylamide and guanine proceeding via Michael addition as presented in **Figure 4**. Because the transition state structure could not be located in vacuo, potential of mean force (pmf) was calculated along the reaction coordinate using the HF/6-31G(d) level of theory in conjunction with the SCRF model. Minima of the pmf represents the reactants and maxima the transition state. Simulation gave an activation energy of 39.92 kcal/mol, a zero-point energy correction of 0.80 kcal/mol, a hydration free energy correction of −12.28 kcal/mol, and consequently the activation free energy

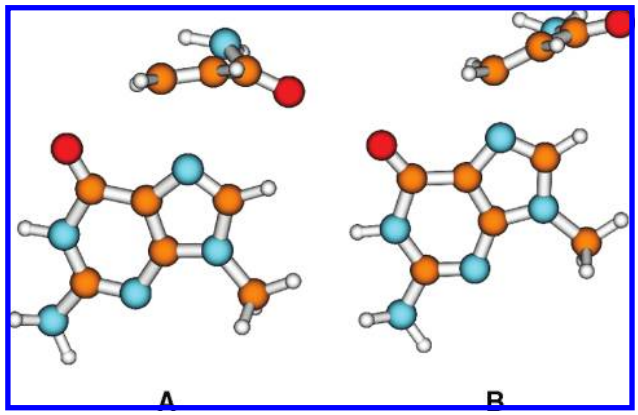

Figure 8. Structures of the reactants (**A**) and the transition state (**B**) for the guanine alkylation by acrylamide calculated at the HF/6-31G(d) level of theory. Oxygen is depicted in red, carbon in orange, nitrogen in blue, and hydrogen in white.

of 28.44 kcal/mol, which is only 0.12 kcal/mol higher than the corresponding barrier for the glycidamide alkylation. It remains a challenge to resolve this issue by carefully performed experimental kinetic studies, because such a small free energy difference might be an artifact of the changed simulation protocol. The structures of the reactants and the transition state for the reaction between acrylamide and guanine calculated at the HF/6-31G(d) level of theory are presented in **Figure 8**. A single imaginary vibrational frequency was obtained for the transition state structure. Its vibration mode coincided with the reaction coordinate of the first step of the reaction mechanism depicted in **Figure 4**—the formation of a chemical bond between the N7 atom of guanine and the first carbon of acrylamide—thus confirming the allocation of the correct transition state structure. The vibration mode of the imaginary frequency obtained at the HF/6-31G(d) level of theory can be viewed as movie 4 included in the Supporting Information.

In this paper, we present quantum chemical simulations of the rate-limiting step of the reaction between guanine and glycidamide—the ultimate carcinogen of acrylamide. We demonstrate that the Møller−Plesset perturbation method of the second order (MP2) combined with the solvent reaction field (SCRF) model and flexible basis sets gives a very good agreement with the experimental activation free energy. The same holds for the Hartree−Fock level of theory in conjunction with the Langevin dipoles (LD) solvation model and flexible basis sets. This agreement presents strong evidence in favor of the validity of the proposed S_N2 reaction mechanism and points to applicability of quantum chemical methods to reactions of carcinogenesis. Insignificant stereoselectivity of the studied alkylation was also predicted. Finally, the competing reaction of glycidamide with adenine was simulated and the experimentally observed regioselectivity was successfully reproduced.

Only some of the available quantum-chemical methods were applied in this study. There is still room to apply QM/MM methodology with all-atom representation of the polar environment and application of thermal averaging (*23, 44−46*). In addition, it would be interesting to test novel DFT functionals (*47*) or to reparametrize the semiempirical methods as reported by Truhlar and co-workers (*48*). Finally, it remains a challenge to study the catalytic effect of microwaves on this class of reactions (*49*).

Carcinogenesis is a complex pathological process by which normal cells are transformed to neoplastic cells. Cell proliferation and apoptosis are physiological processes balanced tightly by proto-oncogenes and antioncogenes. Mutations of these genes along with the genes encoding DNA repair proteins can cause a cell to lose control of proliferation. This results in an uncontrolled cell division and tumor formation (*50*). Carcinogenesis may involve many chemical reactions (*12, 13, 51*) associated with a variety of endogenous and exogenous carcinogens (*52−54*). It is therefore a major challenge to understand and model these reactions (*55−59*). We are sure that such calculations can present an important contribution to the understanding, prevention, and treatment of cancer (*60−63*).

ABBREVIATIONS USED

DFT, density functional theory; MO, molecular orbital; LD, Langevin dipoles; SCRF, solvent reaction field; EVB, empirical valence bond; HF, Hartree−Fock; MP2, Møller−Plesset perturbation of the second order; pmf, potential of mean force.

ACKNOWLEDGMENT

We thank Andrej Perdih from the National Institute of Chemistry and Ana Bergant from the University of Ljubljana for their help with the preparation of the manuscript.

Supporting Information Available: Movie 1 visualizes the reactive mode between glycidamide and guanine; movie 2 depicts the reactive mode between glycidamide and adenine at position N3; movie 3 presents the reactive mode between glycidamide and adenine at position N1; and movie 4 shows the reactive mode between acrylamide and guanine. This material is available free of charge via the Internet at http://pubs.acs.org.

LITERATURE CITED

(1) International Agency for Research on Cancer (IARC). Acrylamide *Summaries and Evaluations*; IARC: Lyon, France, 1994; Vol. 60, pp 389−389.

(2) Rosen, J.; Hellenas, K. E. Analysis of acrylamide in cooked foods by liquid chromatography tandem mass spectrometry. *Analyst* **2002**, *127*, 880–882.

(3) Tareke, E.; Rydberg, P.; Karlsson, P.; Eriksson, S.; Törnqvist, M. Analysis of acrylamide, a carcinogen formed in heated foodstuffs. *J. Agric. Food Chem.* **2002**, *50*, 4998–5006.

(4) Mottram, D. S.; Wedzicha, B. L.; Dodson, A. T. Acrylamide is formed in the Maillard reaction. *Nature* **2002**, *419*, 448–449.

(5) International Agency for Research on Cancer (IARC). Acrylamide *IARC Monograph Series 39*; IARC: Lyon, France, 1982; pp 1−26.

(6) International Agency for Research on Cancer (IARC). Acrylamide *IARC Monograph Series 60*; IARC: Lyon, France, 1995; pp 1−45.

(7) Dixit, R.; Seth, P. K.; Mukjtar, H. Metabolism of acrylamide into urinary mercapturic acid and cysteine conjugates in rats. *Drug Metab. Dispos.* **1982**, *10*, 196–197.

(8) Sumner, S. C.; MacNeela, J. P.; Fennell, T. R. Characterization and quantitation of urinary metabolites of [1,2,3-^{13}C]acrylamide in rats and mice using ^{13}C nuclear magnetic resonance spectroscopy. *Chem. Res. Toxicol.* **1992**, *5*, 81–89.

(9) Sumner, S. C.; Fennell, T. R.; Moore, T. A.; Chanas, B.; Gonzalez, F.; Ghanayem, B. I. Role of cytochrome P450 2E1 in the metabolism of acrylamide and acrylonitrile in mice. *Chem. Res. Toxicol.* **1999**, *12*, 1110–1116.

(10) Calleman, C. J.; Bergmark, E.; Costa, L. G. Acrylamide is metabolized to glycidamide in the rat: evidence from hemoglobin adduct formation. *Chem. Res. Toxicol.* **1990**, *3*, 406–412.

(11) Fuhr, U.; Boettcher, M. I.; Kinzig-Schippers, M.; Weyer, A.; Jetter, A.; Lazar, A.; Taubert, D.; Tomalik-Scharte, D.; Pournara, P.; Jakob, V.; Harlfinger, S.; Klaassen, T.; Berkessel, A.; Angerer, J.; Sörgel, F.; Schömig, E. Toxicokinetics of acrylamide in humans after ingestion of a defined dose in a test meal to improve risk assessment for acrylamide carcinogenicity. *Cancer Epidemiol. Biomarkers Prevention* **2006**, *15*, 266–271.

(12) Segerback, D.; Calleman, C. J.; Schroeder, J. L.; Costa, L. G.; Faustman, E. M. Formation of N-7-(2-carbamoyl-2-hydroxyethyl)guanine in DNA of the mouse and the rat following intraperitoneal administration of [^{14}C]acrylamide. *Carcinogenesis* **1995**, *16*, 1161–1165.

(13) Gamboa da Costa, G.; Churchwell, M. I.; Hamilton, L. P.; Von Tungeln, L. S.; Beland, F. A.; Marques, M. M. DNA adduct formation from acrylamide via conversion to glycidamide in adult and neonatal mice. *Chem. Res. Toxicol.* **2003**, *16*, 1328–1337.

(14) Johnson, W. W.; Guengerich, F. P. Reaction of aflatoxin B1 exo-8,9-epoxide with DNA: kinetic analysis of covalent binding and DNA-induced hydrolysis. *Proc. Natl. Acad. Sci. U.S.A.* **1997**, *94*, 6121–6125.

(15) Doerge, D. R.; da Costa, G. G.; McDaniel, L. P.; Churchwell, M. I.; Twaddle, N. C.; Beland, F. A. DNA adducts derived from administration of acrylamide and glycidamide to mice and rats. *Mutat. Res.* **2005**, *580*, 131–141.

(16) Maniere, I.; Godard, T.; Doerge, D. R.; Churchwell, M. I.; Guffroy, M.; Laurentie, M.; Poul, J. M. DNA damage and DNA adduct formation in rat tissues following oral administration of acrylamide. *Mutat. Res.* **2005**, *580*, 119–129.

(17) Solomon, J. J.; Fedyk, J.; Mukai, F.; Segal, A. Direct alkylation of 2′-deoxynucleosides and DNA following in vitro reaction with acrylamide. *Cancer Res.* **1985**, *45*, 3465–3470.

(18) Solomon, J. J. Cyclic adducts and intermediates induced by simple epoxides. *IARC Sci. Publ.* **1999**, *150*, 123–135.

(19) Johnson, K. A.; Gorzinski, S. J.; Bodner, K. M.; Campbell, R. A.; Wolf, C. H.; Friedman, M. A.; Mast, R. W. Chronic toxicity and oncogenicity study on acrylamide incorporated in the drinking water of Fischer 344 rats. *Toxicol. Appl. Pharmacol.* **1986**, *85*, 154–168.

(20) Friedman, M. A.; Dulak, L. H.; Stedham, M. A. A lifetime oncogenicity study in rats with acrylamide. *Fundam. Appl. Toxicol.* **1995**, *27*, 95–105.

(21) Park, J.; Kamendulis, L. M.; Friedman, M. A.; Klaunig, J. E. Acrylamide-induced cellular transformation. *Toxicol. Sci.* **2002**, *65*, 177–183.

(22) Twaddle, N. C.; McDaniel, L. P.; Gamboa da Costa, G.; Churchwell, M. I.; Beland, F. A.; Doerge, D. R. Determination of acrylamide and glycidamide serum toxicokinetics in B6C3F1 mice using LC-ES/MS/MS. *Cancer Lett.* **2004**, *207*, 9–17.

(23) Warshel, A. *Computer Modeling of Chemical Reactions in Enzymes and Solutions*; Wiley: New York, 1991.

(24) Miertus, S.; Scrocco, E.; Tomasi, J. Electrostatic interaction of a solute with a continuum. A direct utilizaion of ab initio molecular potentials for the prevision of solvent effects. *Chem. Phys.* **1981**, *55*, 117–129.

(25) Florian, J.; Warshel, A. Langevin dipoles model for ab initio calculations of chemical processes in solution: parametrization and application to hydration free energies of neutral and ionic solutes and conformational analysis in aqueous solution. *J. Phys. Chem. B* **1997**, *101*, 5583–5595.

(26) Hawkins, G. D.; Lynch, G. C.; Giesen, D. J.; Rossi, I.; Storer, J. W.; Liotard, D. A.; Cramer, C. J.; Truhlar, D. G. *AMSOL Version 5.4.1*; University of Minnesota: Minneapolis, MN, 1996.

(27) Borštink, U.; Hodošèek, M.; Janežič, D. Improving the performance of molecular dynamics simulations on parallel clusters. *J. Chem. Inf. Comput. Sci.* **2004**, *44*, 359–364.

(28) Borštink, U.; Janežič, D. Symplectic molecular dynamics simulations on specially designed parallel computers. *J. Chem. Inf. Model.* **2005**, *45*, 1600–4.

(29) Frisch, M. J.; Trucks, G. W.; Schlegel, H. B.; Scuseria, G. E.; Robb, M. A.; Cheeseman, J. R.; Montgomery, J. A.; Vreven, T.; Kudin, K. N.; Burant, J. C.; Millam, J. M.; Iyengar, S. S.; Tomasi, J.; Barone, V.; Mennucci, B.; Cossi, M.; Scalmani, G.; Rega, N.; Petersson, G. A.; Nakatsuji, H.; Hada, M.; Ehara, M.; Toyota, K.; Fukuda, R.; Hasegawa, J.; Ishida, M.; Nakajima, T.; Honda, Y.; Kitao, O.; Nakai, H.; Klene, M.; Li, X.; Knox, J. E.; Hratchian, H. P.; Cross, J. B.; Adamo, C.; Jaramillo, J.; Gomperts, R.; Stratmann, R. E.; Yazyev, O.; Austin, A. J.; Cammi, R.; Pomelli, C.; Ochterski, J. W.; Ayala, P. Y.; Morokuma, K.; Voth, G. A.; Salvador, P.; Dannenberg, J. J.; Zakrzewski, V. G.; Dapprich, S.; Daniels, A. D.; Strain, M. C.; Farkas, O.; Malick, D. K.; Rabuck, A. D.; Raghavachari, K.; Foresman, J. B.; Ortiz, J. V.; Cui, Q.; Baboul, A. G.; Clifford, S.; Cioslowski, J.; Stefanov, B. B.; Liu, G.; Liashenko, A.; Piskorz, P.; Komaromi, I.; Martin, R. L.; Fox, D. J.; Keith, T.; Al-Lahram, M. A.; Peng, C. Y.; Nanayakkara, A.; Challachombe, M.; Gill, P. M. W.; Johnson, B.; Chen, W.; Wong, M. W.; Gonzales, C.; Pople, J. A. *Gaussian 03, Revision B02*; Gaussian: Pittsburgh, PA, 2003.

(30) Becke, A. D. Density-functional thermochemistry. III. The role of exact exchange. *J. Chem. Phys.* **1993**, *98*, 5648–5652.

(31) Lee, C.; Yang, W.; Parr, R. G. Development of the Colle−Salvetti correlation-energy formula into a functional of the electron density. *Phys. Rev. B* **1988**, *37*, 785–789.

(32) Garcia-Viloca, M.; Alhambra, C.; Truhlar, D. G.; Gao, J. Hydride transfer catalyzed by xylose isomerase: mechanism and quantum effects. *J. Comput. Chem.* **2003**, *24*, 177–190.

(33) Florian, J.; Warshel, A. Calculations of hydration entropies of hydrophobic, polar, and ionic solutes in the framework of the Langevin dipoles solvation model. *J. Phys. Chem. B* **1999**, *103*, 10282–10288.

(34) Kuhn, B.; Kollman, P. A. QM-FE and molecular dynamics calculations on catechol *o*-methyltransferase: free energy of activation in the enzyme and in aqueous solution and regioselectivity of the enzyme-catalyzed reaction. *J. Am. Chem. Soc.* **2000**, *122*, 2586–2596.

(35) Strajbl, M.; Florian, J.; Warshel, A. Ab initio evaluation of the free energy surfaces for the general base/acid catalyzed thiolysis of formamide and the hydrolysis of methyl thiolformate: a reference solution reaction for studies of cysteine proteases. *J. Phys. Chem. B* **2001**, *105*, 4471–4484.

(36) Klahn, M.; Rosta, E.; Warshel, A. On the mechanism of hydrolysis of phosphate monoesters dianions in solutions and proteins. *J. Am. Chem. Soc.* **2006**, *128*, 15310–15323.

(37) Schaftenaar, G.; Noordik, J. H. Molden: a pre- and post-processing program for molecular and electronic structures. *J. Comput.-Aided Mol. Des.* **2000**, *14*, 123–124.

(38) Cramer, C. J.; Truhlar, D. G. General parameterized SCF model for free energies of solvation in aqueous solution. *J. Am. Chem. Soc.* **1991**, *113*, 8305–8311.

(39) Cramer, C. J.; Truhlar, D. G. AM1-SM2 and PM3-SM3 parameterized SCF solvation models for free energies in aqueous solution. *Science* **1992**, *256*, 213–216.

(40) Miller, J. L.; Kollman, P. A. Solvation free energies of the nucleic acid bases. *J. Phys. Chem.* **1996**, *100*, 8587–8594.

(41) Bren, U.; Martinek, V.; Florian, J. Decomposition of the solvation free energies of deoxyribonucleoside triphosphates using the free energy perturbation method. *J. Phys. Chem. B* **2006**, *110*, 12782–12788.

(42) Florian, J.; Šponer, J.; Warshel, A. Thermodynamic parameters for stacking and hydrogen bonding of nucleic acid bases in aqueous solution: ab initio/ langevin dipoles study. *J. Phys. Chem. B* **1999**, *103*, 884–892.

(43) Barone, V.; Cossi, M.; Tomasi, J. A new definition of cavities for the computation of solvation free energies by the polarizable continuum model. *J. Chem. Phys.* **1997**, *107*, 3210–3221.

(44) Spiegel, K.; Carloni, P.; Rothlisberger, U. Cisplatin binding to DNA oligomers from hybrid Car-Parrinello/molecular dynamics simulations. *J. Phys. Chem. B* **2004**, *108*, 2699–2707.

(45) Carloni, P.; Alber, F. *Quantum Medicinal Chemistry*; Wiley-VCH: Weinheim, Germany, 2003.

(46) Vayner, G.; Houk, K. N.; Jorgensen, W. L.; Brauman, J. I. Steric retardation of S_N2 reactions in the gas phase and solution. *J. Am. Chem. Soc.* **2004**, *126*, 9054–9058.

(47) Zhao, Y.; Truhlar, D. G. Infinite-basis calculations of binding energies for the hydrogen bonded and stacked tetramers of formic acid and formamide and their use for validation of hybrid DFT and ab initio methods. *J. Phys. Chem. A* **2005**, *109*, 6624–6627.
(48) Pu, J.; Ma, S.; Gao, J.; Truhlar, D. G. Small temperature dependence of the kinetic isotope effect for the hydride transfer reaction catalyzed by *Escherichia coli* dihydrofolate reductase. *J. Phys. Chem. B* **2005**, *109*, 8551–8556.
(49) Bren, U.; Kržan, A.; Mavri, J. Microwave catalysis through rotationally hot reactive species. *J. Phys. Chem. A* **2008**, *112*, 166–171.
(50) Underwood, J. C. E. *General and Systematic Pathology*, 3rd ed.; Churchill Livingstone: Edinburgh, U.K., 2000.
(51) Okajima, T.; Shirakawa, Y.; Hashikawa, A. On the reaction of mutagenic aflatoxin B_1 oxide and benz[a]pyrene diol oxide with guanine residue in DNA double helix. *J. Mol. Struct. (THEOCHEM)* **2002**, *581*, 157–166.
(52) Brookes, P.; Lawley, P. D. Evidence for the binding of polynuclear aromatic hydrocarbons to the nucleic acids of mouse skin: relation between carcinogenic power of hydrocarbons and their binding to deoxyribonucleic acid. *Nature* **1964**, *202*, 781–784.
(53) Volk, D. E.; Rice, J. S.; Luxon, B. A.; Yeh, H. J.; Liang, C.; Xie, G.; Sayer, J. M.; Jerina, D. M.; Gorenstein, D. G. NMR evidence for syn−anti interconversion of a trans opened (10*R*)-dA adduct of benzo[*a*]pyrene (7*S*,8*R*)-diol (9*R*,10*S*)-epoxide in a DNA duplex. *Biochemistry* **2000**, *39*, 14040–14053.
(54) Smela, M. E.; Hamm, M. L.; Henderson, P. T.; Harris, C. M.; Harris, T. M.; Essigmann, J. M. The aflatoxin B(1) formamidopyrimidine adduct plays a major role in causing the types of mutations observed in human hepatocellular carcinoma. *Proc. Natl. Acad. Sci. U.S.A.* **2002**, *99*, 6655–6660.
(55) Bren, U.; Guengerich, P.; Mavri, J. Guanine alkylation by the potent carcinogen aflatoxin B1: quantum chemical calculations. *Chem. Res. Toxicol.* **2007**, *20*, 1134–1140.
(56) Kranjc, A.; Mavri, J. Guanine alkylation by ethylene oxide: calculation of chemical reactivity. *J. Phys. Chem. A* **2006**, *110*, 5740–5744.
(57) Huetz, P.; Kamarulzaman, E. E.; Wahab, H. A.; Mavri, J. Chemical reactivity as a tool to study carcinogenicity: reaction between estradiol and strone 3,4-quinones ultimate carcinogens and guanine. *J. Chem. Inf. Comput. Sci.* **2004**, *44*, 310–314.
(58) Baik, M. H.; Friesner, R. A.; Lippard, S. J. Theoretical study of cisplatin binding to purine bases: why does cisplatin prefer guanine over adenine? *J. Am. Chem. Soc.* **2003**, *125*, 14082–14092.
(59) Huetz, P.; Mavaddat, N.; Mavri, J. Reaction between ellagic acid and an ultimate carcinogen. *J. Chem. Inf. Model.* **2005**, *45*, 1564–1570.
(60) Bren, U.; Zupan, M.; Guengerich, F. P.; Mavri, J. Chemical reactivity as a tool to study carcinogenicity: reaction between chloroethylene oxide and guanine. *J. Org. Chem.* **2006**, *71*, 4078–4084.
(61) Huetz, P.; Poux, V. Carcinogenicity of benzo[*a*]pyrene diol epoxide stereoisomers: a linear free energy relationship study. *J. Mol. Struct. (THEOCHEM)* **2006**, *764*, 167–176.
(62) Baik, M. H.; Friesner, R. A.; Lippard, S. J. Theoretical study on the stability of *N*-glycosyl bonds: why does N7-platination not promote depurination? *J. Am. Chem. Soc.* **2002**, *124*, 4495–4503.
(63) Carra, C.; Iordanova, N.; Hammes-Schiffer, S. Proton-coupled electron transfer in DNA−acrylamide complexes. *J. Phys. Chem. B* **2002**, *106*, 8415–8421.

Received for review March 27, 2008. Revised manuscript received July 11, 2008. Accepted July 15, 2008. Financial support from the Slovenian Ministry of Science and Higher Education through Grant P1-0012 is gratefully acknowledged together with the WFS scholarship.

JF800965Y